ADVANCING EARTH AND SPACE SCIENCE

Geophysical Research Letters

RESEARCH LETTER

10.1029/2020GL092049

D. A. Putrasahan and J.-S. von Storch contributed equally to this work.

Key Points:

- Resolving eddies leads to a slightly cooler but energetically consistent response of global mean surface temperature (GMST) to abrupt $4xCO_2$ forcing
- −0.1°C cooler GMST response correlates with stronger heat uptake by eddying mid and deep ocean
- In the deep ocean, resolving eddies results in stronger heat uptake due to larger response of all relevant heat processes

Supporting Information:

Supporting Information may be found in the online version of this article.

Correspondence to:

D. A. Putrasahan,
dian.putrasahan@mpimet.mpg.de

Citation:

Putrasahan, D. A., Gutjahr, O., Haak, H., Jungclaus, J. H., Lohmann, K., Roberts, M. J., & von Storch, J.-S. (2021). Effect of resolving ocean eddies on the transient response of global mean surface temperature to abrupt $4xCO_2$ forcing. *Geophysical Research Letters*, *48*, e2020GL092049. https://doi.org/10.1029/2020GL092049

Received 10 DEC 2020
Accepted 22 MAR 2021

Effect of Resolving Ocean Eddies on the Transient Response of Global Mean Surface Temperature to Abrupt $4xCO_2$ Forcing

D. A. Putrasahan[1], O. Gutjahr[1], H. Haak[1], J. H. Jungclaus[1], K. Lohmann[1], M. J. Roberts[3], and J.-S. von Storch[1,2]

[1]Max Planck Institute for Meteorology, Hamburg, Germany, [2]Center for Earth System Research and Sustainability (CEN), Universität Hamburg, Hamburg, Germany, [3]Met Office Hadley Centre, Exeter, UK

Abstract The magnitude of global mean surface temperature (GMST) response to increasing atmospheric CO_2 concentrations is affected by the efficiency of ocean heat uptake, which in turn can be affected by oceanic mesoscale eddies. Using the Max Planck Institute - Earth System Model (MPI-ESM1.2), we find that resolving eddies leads to a −0.1°C cooler response of GMST to an abrupt CO_2 quadrupling, which is related to a larger rate of heat uptake by an eddying ocean. This is consistent with changes in the energy budget of the whole climate system induced by increasing ocean resolution under the same radiative forcing and climate feedback. As a fast response, heat is taken up by the deep ocean, independent of resolution. The change in deep ocean heat uptake due to resolved eddies is an amplification in the magnitude of the responses of all heat processes, including eddy heat advection, mean heat advection, and diffusive processes.

1. Introduction

Oceanic mesoscale eddies, which are often parameterized in state-of-the-art climate models, represent an uncertainty source for climate change projections (Winton et al., 2014). This uncertainty is difficult to systematically evaluate mainly because climate models having an oceanic component capable of resolving mesoscale eddies are demanding to produce. This computational burden makes climate change simulations with an eddy-resolving ocean model challenging. While challenging, we present here a set of idealized climate change simulations with the same atmospheric model at the same resolution but differing ocean resolutions, and the experiment is specifically designed for quantifying the main effect of mesoscale eddies on transient climate responses.

The conjecture that mesoscale eddies are capable of affecting transient climate response stems from the knowledge that the climate response is closely linked to the efficiency of the ocean in uptaking heat (Rose & Rayborn, 2016; Winton et al., 2010). Furthermore, the ocean's heat uptake can be affected by oceanic mesoscale eddies as they can significantly contribute to the ocean heat budget (Griffies et al., 2015; Morrison et al., 2013; von Storch et al., 2016; Wolfe et al., 2008). Studies using eddy-permitting/resolving simulations show that to the first order, the downward heat transport due to mean advection is balanced by the upward eddy heat flux, which, when integrated globally, can reach up to 1 to 3 PW (Griffies et al., 2015; Morrison et al., 2013; von Storch et al., 2016; Wolfe et al., 2008). While the effect of mesoscale eddies is typically parameterized, the effect of parameterized eddies can deviate from that of resolved eddies (Griffies et al., 2015; von Storch et al., 2016). Thus, those climate change projections using current generation climate models, which generally rely on eddy parameterizations, potentially suffer from an uncertainty in the ocean heat uptake due to the difference between resolved and parameterized eddies. Consequently, the climate response to changes in greenhouse gas forcing (GHG) can differ in climate models with an eddy-resolving ocean as compared to a non-eddy-resolving ocean. Here, we investigate the effects of mesoscale eddies on the transient climate response, quantified by the change in global mean surface temperatures (GMST, also denoted by T_s) to strong greenhouse gas forcing, and the role of ocean mesoscale eddies in determining the GMST response.

10.1029/2020GL092049

2. Experimental Setup

In order to clearly identify the effect of mesoscale eddies, we choose to consider a strong-forcing scenario, that of an abrupt quadrupling of CO_2 concentration (abrupt-4xCO_2). We use pairs of simulations consisting of a 1950-control (CTL) simulation forced by fixed-1950 GHG-forcing, and an abrupt-4xCO_2 simulation forced by quadrupling CO_2 concentration in 1950. The length of each run after spin up is 100 years. We choose to define CTL using 1950 rather than the canonical 1850 pre-industrial condition, since the work is initiated within the EU project PRIMAVERA and follows the HighResMIP protocol (Haarsma et al., 2016).

We use the Max Planck Institute - Earth System Model (MPI-ESM1.2; Mauritsen et al., 2019; Müller et al., 2018) with the atmospheric component ECHAM6.3 (Stevens et al., 2013) and the oceanic/sea-ice component Max Planck Institute Ocean Model (MPIOM; Jungclaus et al., 2013). We employ two coupled model configurations of MPI-ESM1.2 with the same T127 (~1°) atmospheric resolution, but different ocean resolutions. The effect of ocean eddies is distilled from the two differing ocean horizontal resolutions: The first one has a nominal resolution of 0.1° (Gutjahr et al., 2019) and is eddy-resolving with respect to the first baroclinic Rossby radius of deformation and hereafter referred to as ER (Eddy Rich), but exceptions occur at polar latitudes (Chelton et al., 1998; Hallberg, 2013), in northern subpolar regions and in shallow waters such as shelf areas (Nurser & Bacon, 2014). The second one has a nominal resolution of 0.4° (Müller et al., 2018) and does not resolve eddies at higher latitudes, and is henceforth deemed non-eddy resolving and hereafter referred to as EP (Eddy Poor). This configuration is officially called higher-resolution version of the MPI-ESM1.2 (MPI-ESM1.2-HR; Müller et al., 2018) and is normally referred to as HR. However, to prevent confusion when comparing to ER, we denote it here as EP. Note that MPIOM is formulated on a tripolar grid, which has a rather uniform resolution in the northern hemisphere and a longitude-latitude grid south of the Equator. For ER, the grid size is reduced to about 7 km at 50°S, about 5 km around 70°S, and about 3 km in the Weddell and Ross seas. In both ER and EP, we use a total of 40 z-levels with partial bottom cells. The layer thickness ranges from about 10 m in the first hundred meters, down to about 200–300 m between 1,000 to 3,400 m depth, and about 400–550 m, which is the thickest bottom layer, below 3,500 m.

Since the aim of our study is to understand the effect of resolving mesoscale eddies and not calibrating the climate, we employ, whenever possible, the same parameterizations. In both ER and EP, we use the Redi-parameterization (Redi, 1982) with the same resolution-dependent coefficient of 1,000 m^2/s for a 400 km grid size, which corresponds to about 25 m^2/s in ER and about 100 m^2/s in EP. Thus, the isopycnal eddy-induced mixing can be considered to be essentially resolved in ER, as the Redi-coefficient is extremely small in ER, and represented by the Redi-parameterization in EP. The only differently employed parameterization is the GM-parameterization (Gent & Mcwilliams, 1990) used to represent the effect of mesoscale eddies on tracer advection, which is switched on in EP but switched off in ER. The thickness diffusivity used in EP is 250 m^2s^{-1} for a 400 km grid size that scales linearly with the grid cell size. This number, which is normally used in the MPI-ESM simulations for Coupled Model Intercomparison Project (CMIP) applications (Gutjahr et al., 2019; Jungclaus et al., 2013; Müller et al., 2018), is much smaller than those adopted by other models (about 1000 m^2s^{-1} for a one-degree grid cell size). Several studies that diagnose differences between models may reflect differences between different GM implementations such as varying versus fixed GM coefficients (Kuhlbrodt & Gregory, 2012; Saenko et al., 2018). Here, since EP uses such a small thickness diffusivity, this leads to minute tendencies from GM (von Storch et al., 2016) and thus rendering the eddy-parameterized transports to be negligible. Hence, the difference between ER and EP describes essentially the effect of resolved eddies, rather than the difference between resolved versus parameterized eddies.

One main difficulty in performing climate change simulations using an eddy-resolving model is that due to the heavy computational costs, the spin up runs are often too short such that the simulations following the spin up are afflicted by drifts. In this study, the spin up run is 30 years. We deal with possible drifts by branching off 4xCO_2 simulations from a control simulation, and running the control and 4xCO_2 simulations side by side. By doing so, we assume that the pair of CTL and 4xCO_2 runs would have the same drift. This drift can thus be effectively removed by defining the response in a given year as the difference between 4xCO_2 and CTL in that year.

10.1029/2020GL092049

While we are able to remove the drift in the aforementioned manner, another difficulty arises: That of internal variability. Although internal variability may not play a big role for identifying the response to a strong GHG forcing (defined as the difference between 4xCO_2 and CTL), it can notably contaminate the resolution effect (defined as the difference between high- and low-resolution runs). We tackle this issue by using three ensemble members, each being a set consisting of CTL and 4xCO_2 runs at low and high resolutions. Utilizing a larger ensemble would certainly help to ease this issue more, but this is currently not affordable.

Since we quantify climate response in terms of GMST, which reflects the large-scale internal climate mode El Niño - Southern Oscillation (ENSO), the resolution effect on GMST response can be affected by ENSO events occurring in the runs. We reduce the impact of ENSO by carefully selecting the year we branched off for the 4xCO_2 simulations. However, we realized the impact of ENSO from our first pair of EP and ER 4xCO_2 runs, which were unintentionally branched off from a warm ENSO state for EP and a neutral ENSO state for ER. We then decide to branch off the two additional EP 4xCO_2 runs from a cold and a neutral ENSO state, and ER from all neutral ENSO state, to ensure ENSO-neutral initial conditions.

For this study, a response for any given quantity is computed for each resolution as

$$\mathrm{ER}_{\mathrm{resp}} = \mathrm{ER}_{4\mathrm{xCO}_2} - \mathrm{ER}_{\mathrm{CTL}};\ \mathrm{EP}_{\mathrm{resp}} = \mathrm{EP}_{4\mathrm{xCO}_2} - \mathrm{EP}_{\mathrm{CTL}} \tag{1}$$

and the effect of ocean resolution, denoted as Δ, on the response is evaluated as

$$\Delta = \mathrm{ER}_{\mathrm{resp}} - \mathrm{EP}_{\mathrm{resp}}. \tag{2}$$

Both responses ($\mathrm{ER}_{\mathrm{resp}}$ and $\mathrm{EP}_{\mathrm{resp}}$) and resolution effects (Δ) are calculated from yearly data and then averaged or running averaged over 10 years. For the time rate of change of heat content, the time derivative is calculated using monthly data and then averaged. Taking the decadal mean or applying a 10 years running mean to the response further reduces noise from internal variability and enhances the signal, thereby providing robustness to the response estimate. In our analysis, only ensemble mean statistics are considered.

3. Interpretation Based on the Energy Budget of the Coupled System

The red solid line in Figure 1a (the dashed lines will be discussed later in section 5) shows the 10-years running-average ensemble-mean time series of the resolution effect on GMST response, ΔT_s. We computed GMST based on surface temperature over land, sea-ice, and ocean, and not the traditional Intergovernmental Panel on Climate Change (IPCC) definition that uses near-surface temperature over land and sea-ice (IPCC, 2013). The resolution effect on GMST response is negative throughout the simulation period, indicating that the GMST warms less for a climate with an eddying ocean than for a climate in which mesoscale eddies are not well resolved. When decomposing this resolution effect into contributions from land and ocean surface (Figure S2), we find that land surface temperature and sea surface temperature (SST) contribute more or less equally to ΔT_s, but reveal different variability behaviors. While the contribution from the ocean surface is essentially responsible for the multi-decadal variations seen in Figure 1a, the contribution from land reveal little variations throughout time. The total resolution effect amounts to −0.1°C when averaged over the entire simulation period and reaches a maximum of about −0.2°C.

Performing a one-sided two-sample t-test using a sample size of $n = 3$ (3 ensemble members) suggests that ΔT_s is not statistically significant (gray line in Figure 1a, which marks $c_{0.95}\sqrt{2/n}S_p$ with $c_{0.95}$ being the 95% percentile of the t-distribution, S_p the pooled ensemble standard deviation). Although disappointing, the test result cannot be taken as a proof that mesoscale eddies have no effect on GMST response. This is because the power of a t-test depends on the sample size and is less when the sample size is small (von Storch & Zwiers, 1999). Increasing the sample size can help. However, since the GMST responses represent trends which increase logarithmically with time throughout the simulation period, bootstrapping one ensemble member cannot produce iid (independent, identically distributed) realizations. Instead, the sample size has to be increased by increasing the number of independent ensemble members, which is limited by computational resources. In this situation, a small statistically insignificant value of ΔT_s can imply that there is no resolution effect at all, or that there is a resolution effect but that the sample size is too small for a significant

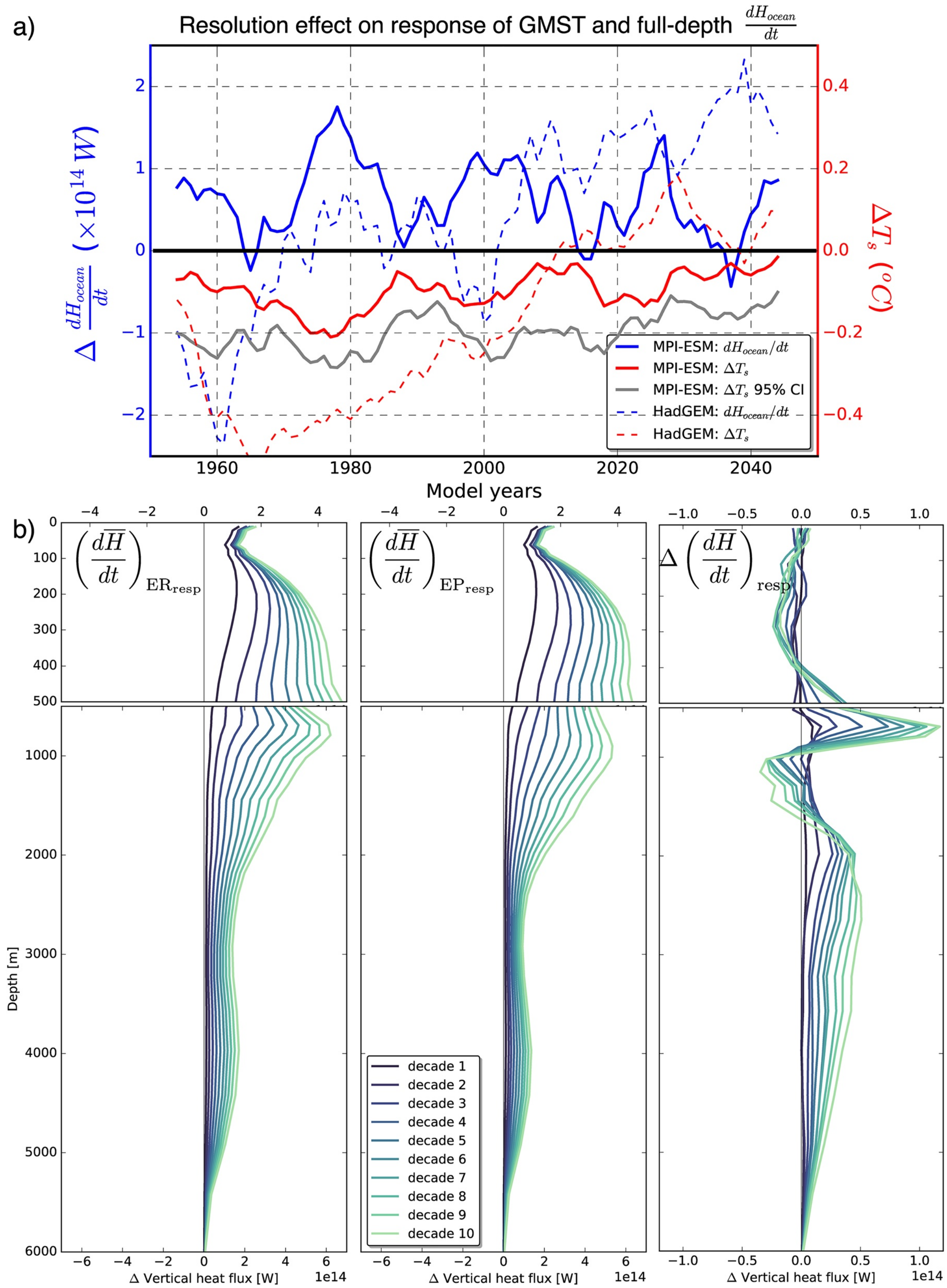
a)
Resolution effect on response of GMST and full-depth $\frac{dH_{ocean}}{dt}$
$\Delta \frac{dH_{ocean}}{dt}$ $(\times 10^{14} W)$
ΔT_s (^oC)
Model years
MPI-ESM: dH_{ocean}/dt
MPI-ESM: ΔT_s
MPI-ESM: ΔT_s 95% CI
HadGEM: dH_{ocean}/dt
HadGEM: ΔT_s
b)
$\left(\frac{d\overline{H}}{dt}\right)_{\mathrm{ER_{resp}}}$
$\left(\frac{d\overline{H}}{dt}\right)_{\mathrm{EP_{resp}}}$
$\Delta\left(\frac{d\overline{H}}{dt}\right)_{\mathrm{resp}}$
Depth [m]
Δ Vertical heat flux [W]
1e14
decade 1
decade 2
decade 3
decade 4
decade 5
decade 6
decade 7
decade 8
decade 9
decade 10

signal to be detected. In this case, we must look for physical significance, i.e., a physical process that can explain the signal.

To assess the physical significance of the resolution effect, we consider a zero-dimensional model of the type studied by (Gregory et al., 2004). This model describes the energy budget of the whole climate system, including the atmosphere, the land, and the ocean: The time rate of change of the heat content of the whole climate system is determined by the radiative forcing and the radiative feedback that is found to be proportional to the surface temperature. When considering only the response to a change in GHG forcing, this energy budget can be written as

$$\frac{dH_{\text{climate}}}{dt} = F - \alpha T_s, \tag{3}$$

where the subscript $_{\text{resp}}$ introduced in Equation 1 is dropped for the sake of brevity. dH_{climate}/dt is the response of the time rate of change in the heat content of the whole system, F represents the forcing change due to the increase in CO_2 concentration, αT_s with the climate feedback parameter $\alpha > 0$, and the GMST response, T_s, represents the radiative feedback in the coupled system. We assume that the heat capacity of the atmosphere can be neglected relative to that of the ocean, and that there is no heat penetrating into the solid earth, such that dH_{climate}/dt of Equation 3 reduces to the response of the time rate of change in the heat content of the ocean, dH_{ocean}/dt. The negative sign in Equation 3 describes the situation that for the same F, the larger T_s, the stronger the negative feedback (mainly due to back radiation to space), and the smaller the dH_{climate}/dt. When subtracting the budget for EP from the budget for ER, and assuming that F and α remain the same, one finds

$$\Delta \frac{dH_{\text{ocean}}}{dt} = -\alpha \Delta T_s. \tag{4}$$

$\Delta\left(dH_{\text{ocean}} / dt\right)$ and ΔT_s denote the resolution effects on the response of time rate of change in ocean heat content and on that of GMST, respectively. Figure S1 in SI suggests that α and F are indeed essentially unchanged from ER to EP. This likely results from the fact that ER and EP use the same atmospheric model with the same resolution subjected to the same 4xCO_2 forcing.

Equation 4 suggests that the resolution effect for GMST, ΔT_s, should be in antiphase with that of ocean heat uptake response, $\Delta\left(dH_{\text{ocean}} / dt\right)$. Figure 1a shows that such an anti-phase relationship between ΔT_s (red solid line) and $\Delta\left(dH_{\text{ocean}} / dt\right)$ (blue solid line) can indeed be identified: A larger response of time rate of change of ocean heat content in ER than in EP is generally associated with a smaller GMST response in ER than in EP. We therefore conclude that although small, the resolution effect for GMST is clearly physically significant and can be explained in terms of the zero-dimensional energy budget of the coupled system.

4. Further Interpretation Using Vertical Heat Budget of the Ocean

When using the time rate of change in heat content response as an indicator for ocean heat uptake response (hereon dH/dt), the positive resolution effect for dH/dt suggests that an eddying ocean takes up more heat under 4xCO_2 forcing compared to an ocean that does not resolve eddies. To address the role of mesoscale eddies for this ocean heat uptake response, in particular to understand where and how heat is taken up in ER and EP, we examine the vertical structures of dH/dt and the contributing heat processes by considering the global heat budget of each ocean layer k:

Figure 1. (a) 10 years running mean of the resolution difference (ER-EP) in GMST response (red line) and rate of change of ocean heat content (blue line), for MPI-ESM 4xCO_2 simulations (solid) and HadGEM3-GC31 historical and SSP5-8.5 simulations (dashed). Gray line marks the value, below which the resolution difference is significant at 5% significance level, based on a one-sided t-test with sample size being 3. (b) Ensemble mean depth profile of the response of rate of change in global ocean heat content $\left(d\overline{H} / dt\right)_{\text{resp}}$ in ER (leftmost panel), in EP (middle panel), and for ER-EP (rightmost panel). Color shading from dark blue to light green shows progression of each profile on decadal interval. Each decade is accumulated upon the previous decade to show the integrated effect over time. EP, Eddy Poor; ER, Eddy Rich; GMST, global mean surface temperature; HadGEM3-GC31, Hadley Centre Global Environment Model in the Global Coupled configuration 3.1; MPI-ESM, Max Planck Institute - Earth System Model; SSP, shared socio-economic.

$$\frac{d\overline{H_k}}{dt} = \rho_o C_p \left(\frac{\delta(\overline{wT})}{\delta z} \right)_k + \overline{D_k} \tag{5}$$

where $\overline{\text{overbar}}$ indicates decadal mean, ρ_o is the reference density of seawater, C_p is the specific heat capacity of water, $\rho_o C_p \left(\frac{\delta(\overline{wT})}{\delta z} \right)_k$ is the vertical heat flux convergence of the kth layer, $\overline{D_k}$ includes diffusive terms in the kth layer that encompasses vertical mixing, convection, isopycnal mixing (Redi parameterization), and also incorporates penetrative shortwave radiation and surface heat flux in the surface layer. The vertical flux convergence term can be decomposed into a mean and eddy component such that Equation 5 can be expressed as:

$$\begin{aligned} \frac{d\overline{H_k}}{dt} &= \rho_o C_p \left(\frac{\delta(\overline{w}\overline{T})}{\delta z} \right)_k + \rho_o C_p \left(\frac{\delta(\overline{w'T'})}{\delta z} \right)_k + \overline{D_k} \\ &= \overline{M_k} + \overline{E_k} + \overline{D_k} \end{aligned} \tag{6}$$

where indicates deviations from the respective $\overline{\text{overbar}}$, $\overline{M_k}$ is the vertical heat flux convergence due to mean flow, and $\overline{E_k}$ is the vertical heat flux convergence due to eddying flow. The response in the rate of change of global ocean heat content can thus be expressed as:

$$\begin{aligned} \left(\frac{d\overline{H_k}}{dt} \right)_{\text{resp}} &= \underbrace{\left(\overline{M_{k,4\text{xCO}_2}} - \overline{M_{k,\text{CTL}}} \right)}_{\text{response of } \textbf{mean} \text{ vertical flux}} + \underbrace{\left(\overline{E_{k,4\text{xCO}_2}} - \overline{E_{k,\text{CTL}}} \right)}_{\text{response of } \textbf{eddy} \text{ vertical flux}} + \underbrace{\left(\overline{D_{k,4\text{xCO}_2}} - \overline{D_{k,\text{CTL}}} \right)}_{\text{response of diffusive terms}} \\ &= \overline{M_{k,\text{resp}}} + \overline{E_{k,\text{resp}}} + \overline{D_{k,\text{resp}}} \end{aligned} \tag{7}$$

where $\overline{M_{k,\text{resp}}}$ is the response of the mean vertical heat convergence, $\overline{E_{k,\text{resp}}}$ is the response of the eddy vertical heat convergence, and $\overline{D_{k,\text{resp}}}$ is the response of the diffusive terms. The resolution effect (Δ) on each term in Equation 7 can then be expressed as

$$\Delta \left(\frac{d\overline{H_k}}{dt} \right)_{\text{resp}} = \Delta \overline{M_{k,\text{resp}}} + \Delta \overline{E_{k,\text{resp}}} + \Delta \overline{D_{k,\text{resp}}} \tag{8}$$

Generally, $\overline{E}$ contains contributions from resolved fluctuations w' and T', denoted as E_χ. For EP, it contains also the contribution from the GM parameterization. We assess the contribution from the GM-parameterization and find that except for the surface layer, it is much less than E_χ, consistent with the results from the stand-alone MPIOM simulations (von Storch et al., 2016). The smallness of the GM-contribution further confirms that the difference between ER and EP describes essentially the effect of resolved eddies, rather than resolved versus parameterized eddies. Hereafter, our computation of E will be $E = E_\chi = \rho_o C_p \delta(\overline{w'T'})$ for both ER and EP.

To address the question where in the water column is heat most efficiently taken up, we consider for each subsequent decade, the vertical structures of $\left(d\overline{H_k} / dt \right)_{\text{resp}}$ in ER and EP, and the difference between the two (Figure 1b). In both ER and EP (left and middle panel), a local minima of ocean heat uptake occurs at 70–100 m depth and a maximum between 600–1,100 m depth. Below 2,000 m, heat uptake is less than a third of that is seen in the upper 1,000 m, and yet the difference between ER and EP is comparatively considerable (right panel of Figure 1b).

While the largest positive values of $\Delta\left(d\overline{H_k} / dt \right)_{\text{resp}}$ occur between 500–1,000 m, there are appreciable negative values right below, between 1,000–1,800 m (right panel in Figure 1b). This dipole-like structure arises from the different depths of maximum $\left(d\overline{H_k} / dt\right)_{\mathrm{resp}}$: i.e., ~700 m in ER (left), but ~1,000 m in EP (middle). The dipole-like structure implies a compensation, leaving the greater $\Delta\left(d\overline{H_k} / dt\right)_{\mathrm{resp}}$ in the deep ocean as the main signal responsible for the positive resolution effect $\Delta\left(dH_{\mathrm{ocean}} / dt\right)$ for the entire ocean shown in Figure 1a. Therefore, to address the question of how eddy heat flux affects the heat uptake, we now focus on the deep ocean, henceforth considering profiles at depths below 2,000 m.

We start by considering the full states, rather than the responses. Figures 2a and 2b show profiles of the heat budget terms in the deep ocean from the $4xCO_2$ simulations, resulting from Equation 6. The ER profiles (top panel) are similar to the EP profiles (middle panel). Between ~2,000–4,000 m, mean heat advection, $\left(\overline{M_k}\right)_{4xCO_2}$ (second column), dominates over $\left(\overline{D_k}\right)_{4xCO_2}$ and $\left(\overline{E_k}\right)_{4xCO_2}$ (first and third column). Below 4,000 m, diffusive processes, $\left(\overline{D_k}\right)_{4xCO_2}$, dominates over $\left(\overline{M_k}\right)_{4xCO_2}$ and $\left(\overline{E_k}\right)_{4xCO_2}$. Throughout the deep ocean, the profile of mean heat advection, $\left(\overline{M_k}\right)_{4xCO_2}$, and diffusive processes, $\left(\overline{D_k}\right)_{4xCO_2}$, are of opposite signs, which is in line with the one-dimensional advection/diffusion balance in the abyssal ocean (Munk & Wunsch, 1998) hypothesized by Munk (1966), albeit without eddy flux consideration. The profiles also reveal that eddy heat flux divergence $\left(\overline{E_k}\right)_{4xCO_2}$ (third column) acts only in one direction in the deep ocean, that is to reduce the rate of heat absorption. All three terms, $\left(\overline{D_k}\right)_{4xCO_2}$, $\left(\overline{M_k}\right)_{4xCO_2}$ and $\left(\overline{E_k}\right)_{4xCO_2}$, are larger than $\left(d\overline{H_k} / dt\right)_{4xCO_2}$ (right column).

One important feature of heat uptake in both ER and EP is that positive values of $\left(d\overline{H_k} / dt\right)_{4xCO_2}$ are already found down to the ocean bottom in the first decade (dark blue profiles in the right column in Figures 2a and 2b). These initial increases persist and visually remains unchanged in the following decades, which leads to an approximately steady warming. The warming below 2,000 m occurs predominantly in the mid- to high-latitude oceans (Figure S3). We speculate that this initial deep warming is due to the advection related to mean vertical velocity and vertical mixing induced by vertical velocity fluctuations. Figure S4 (lower panel) shows that the mean vertical velocity can occasionally reach $O\,(10^{-5})$ m/s in the upper ocean and up to $O\,(10^{-4})$ m/s in the deep ocean in both ER and EP, although this velocity is clearly stronger in ER than in EP. When ignoring all other processes, a mean vertical velocity of $O\,(10^{-5})$ m/s alone can transport a surface signal down to about 3,000 m within a decade. Thus, the mean vertical velocity is, at least in principle, capable of transporting a surface signal down to a few km within one decade. Thus far, the consideration is focused on Eulerian vertical velocity, which is only a part of the effective (or residual) velocity directly related to tracer advection. The other part is the eddy-induced velocity. Liang et al. (2017) show that the effective velocity is primarily driven by the Eulerian vertical velocity. Their results indicate that taking eddy-induced velocity into account will likely not change the broad picture. Figure S4 shows further (upper panel) that the magnitudes of the vertical velocity fluctuations are much larger than those of the mean vertical velocities, and the strongest fluctuations tend to be located in the same mid- and high-latitude oceans where deep warming is found. These fluctuations can be generated by baroclinic instability that converts available potential energy to eddy kinetic energy, and by fluctuating winds that excite near-inertial motions and/or induce Ekman-type of velocity fluctuations. Both baroclinic instability and fluctuating wind forcing are present in ER, but only fluctuating winds take effect in EP. Thus, velocity fluctuations are much stronger in ER than in EP. These fluctuations can further reinforce the transport or mixing of the surface signal down to the deep ocean. Consistent with that, the warming penetrates somewhat deeper in ER than in EP (Figure S3). The warming below 2,000 m is accompanied by a constant adjustment of $\left(\overline{D_k}\right)_{4xCO_2}$, $\left(\overline{M_k}\right)_{4xCO_2}$ and $\left(\overline{E_k}\right)_{4xCO_2}$ (left three panels of Figures 2a and 2b): The magnitudes of all three terms decrease progressively with increasing time, suggesting that the heat processes become increasingly less vigorous.

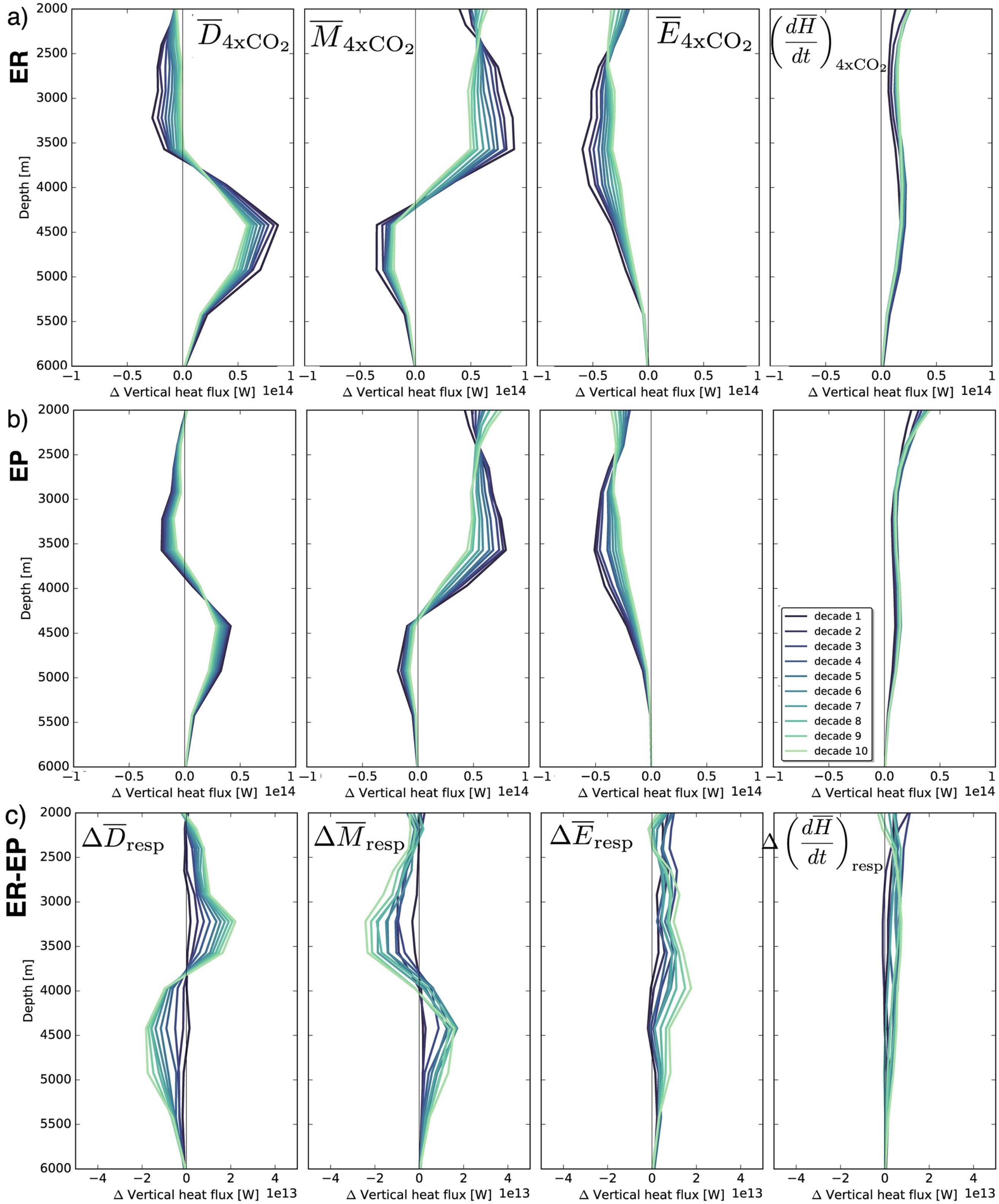
a)
ER
$\overline{D}_{4xCO_2}$
$\overline{M}_{4xCO_2}$
$\overline{E}_{4xCO_2}$
$\left(\frac{d\overline{H}}{dt}\right)_{4xCO_2}$
b)
EP
c)
ER-EP
$\Delta\overline{D}_{resp}$
$\Delta\overline{M}_{resp}$
$\Delta\overline{E}_{resp}$
$\Delta\left(\frac{d\overline{H}}{dt}\right)_{resp}$
Depth [m]
Δ Vertical heat flux [W] 1e14
Δ Vertical heat flux [W] 1e13
decade 1
decade 2
decade 3
decade 4
decade 5
decade 6
decade 7
decade 8
decade 9
decade 10

The temporal decrease in the vigorousness of the heat processes behind $\left(\overline{D_k}\right)_{4\text{xCO}_2}$, $\left(\overline{M_k}\right)_{4\text{xCO}_2}$, and $\left(\overline{E_k}\right)_{4\text{xCO}_2}$ corresponds to a temporal increase in the magnitudes of responses $\left(\overline{D_k},\right)_{\text{resp}}$, $\left(\overline{M_k},\right)_{\text{resp}}$, and $\left(\overline{E_k},\right)_{\text{resp}}$. Although both models exhibit increases in the response magnitudes with time, the increase in magnitude of ER response is larger (Figure 2c). More specifically, the resolution effects on the diffusive processes and mean heat flux (first two panels of Figure 2c) seem to cancel out, while the resolution effect on the eddy heat flux (third panel of Figure 2c) is generally only positive. The sum of the resolution effects on all three heat processes below about 2,500 m is somewhat stronger in ER than in EP, meaning that the presence of eddies amplifies the magnitude of all heat process responses (i.e., a stronger reduction in the vigorousness of all heat processes in an eddying ocean), resulting in positive values of $\Delta\left(d\overline{H_k} / dt\right)_{\text{resp}}$ throughout most of the deep ocean (rightmost panel in Figure 2c). Apart from eddies, the better resolved mean flows and bathymetric features in ER can also contribute to the amplification of heat processes. How big this contribution is relative to that from eddies is unclear and needs to be further investigated.

In summary, the following picture emerges. At first approximation, the deep ocean already begins to take up heat in the first decade, probably due to the vertical mixing related to vertical velocity fluctuations, and the uptake continues at a roughly constant rate throughout the integration time. Furthermore, as more heat is taken up, all heat processes gradually weaken. The weakening could be a consequence of the ocean becoming increasingly more stable under the 4xCO_2 forcing. This weakening, however, needs to be further investigated. The above first-order picture is independent of resolution. With a closer examination of the responses and the resolution effects, differences between ER and EP in the deep ocean become more apparent. The heat uptake below 2,000 m is stronger in ER than in EP. This resolution effect is manifested in a stronger reduction with time in the vigorousness of all heat processes (diffusive processes, mean and eddy vertical heat advection) in ER compared to that in EP.

5. Discussion

5.1. Heat Uptake in the Upper, Mid and Deep Ocean

Although this paper concentrates on the heat uptake in the deep ocean, where the resolution effect on the heat content of the ocean as a whole resides, resolving eddies impacts the heat uptake throughout the water column (Figure 1b). In the upper few hundred meters, the ocean takes up less heat in ER than in EP, corresponding to a cooler global mean SST, and with that a cooler GMST in ER than in EP. In the mid ocean from about 500 to 1,500 m, the maximum of heat uptake response is shifted by about 200–300 m from about 1,000 m in EP to about 700 m in ER (left and middle panels of Figure 1b), resulting in a dipole structure in $\Delta\left(d\overline{H} / dt\right)_{\text{resp}}$ (right panel of Figure 1b) with positive values centered near 700 m and negative values below 900 m. Since the positive values are larger than the negative ones, the mid ocean from 500 to 1,500 m takes up more heat in ER than in EP. The upward shift of the maximum of heat uptake response from EP to ER could be caused by the more strongly enhanced stratification in the tropical ocean between 600 and 1,000 m in ER than in EP (Figure S3b). In the deep ocean (below 2,000 m), the heat uptake is enhanced more uniformly throughout the depth in ER relative to EP.

5.2. Resolution Effect on GMST-Response in Other Climate Change Simulations

Climate change experiments have also been carried out using other climate models with an eddy-resolving ocean. For instance, the experiments at the Hadley Centre consist of historical simulations (1950–2014) and subsequent shared socio-economic (SSP5-8.5) scenario forced runs (O'Neill et al., 2016) for 2015–2050

Figure 2. (a) & (b) Ensemble mean depth profiles of ocean heat budget terms in the deep ocean following Equation 6 and specifically for only 4xCO_2 simulations. Top panel corresponds to ER while middle panel corresponds to EP. Leftmost panel is for diffusive terms ($\overline{D}_{4\text{xCO}_2}$), second column for mean vertical temperature flux convergence ($\overline{M}_{4\text{xCO}_2}$), third column for eddy vertical temperature flux convergence ($\overline{E}_{4\text{xCO}_2}$), and rightmost panel for $\left(d\overline{H} / dt\right)_{4\text{xCO}_2}$ (c) Effect of resolution on depth profiles of ocean heat budget terms following Equation 8. Same as (a) & (b) except that they are profiles of the resolution effect on the response to 4xCO_2, i.e., $\Delta = \text{ER}_{\text{resp}} - \text{EP}_{\text{resp}}$, where resp = 4x$CO_2$ - CTL. Color shading from dark blue to light green shows decadal progression of each profile. Unlike Figure 1b, profiles are not accumulated for each decade.

10.1029/2020GL092049

in a high-resolution setup (Hadley Centre Global Environment Model in the Global Coupled configuration 3.1 high resolution (HadGEM3-GC31-HH)) that uses a 1/12° ocean and a 50 km atmosphere, and a low resolution setup (Hadley Centre Global Environment Model in the Global Coupled configuration 3.1 low resolution (HadGEM3-GC31-LL)) that uses a 1° ocean and a 250 km atmosphere (Roberts et al., 2019). On Figure 1a, the resolution effect for GMST response (red dashed line) and the resolution effect for response of the time rate of change of total heat content (blue dashed line) derived from HadGEM3-GC31 experiments are shown. Different from MPI-ESM simulations (solid lines), there is no clear anti-phase relation between $\Delta\left(dH_{\text{ocean}} / dt\right)$ and ΔT_s. Quite the contrary, from about 2020 onward, when CO_2 concentration is further enhanced relative to the historical period, ΔT_s and $\Delta\left(dH_{\text{ocean}} / dt\right)$ are both positive.

Although it is beyond the scope of this paper to rigorously examine the reasons for the different resolution effects, there are two candidates worth mentioning. The first one is the different types of resolution change. While only oceanic resolution is increased in MPI-ESM experiments, both atmospheric and oceanic resolution are increased in HadGEM3-GC31 experiments. In the framework of the energy balance model (Equation 3), the climate feedback parameter α is determined by radiative feedbacks, such as water vapor and lapse rate feedbacks, which strongly depend on the atmospheric state. Deploying different atmospheric resolutions such as in HadGEM3-GC31 experiments can lead to different atmospheric states and from that different α. A resolution dependent α not only prevents the anti-phase relation between $\Delta\left(dH_{\text{ocean}} / dt\right)$ and ΔT_s to be established, it also makes the interpretation of the resolution effect difficult, since this effect can then be induced by resolving ocean eddies as well as by changing climate feedbacks.

The second candidate is the different radiative forcings. Equation 3 can be decomposed into two budgets, one for the atmosphere and the upper ocean and the other for the deep ocean. Geoffroy et al. (2013) show that the solution of this two layer model depends strongly on the forcing imposed. The solution is dominated by a fast response for a step forcing, which is used in MPI-ESM experiments. However, the solution follows closely the evolution of the forcing for a linear forcing, which resembles the forcing used in HadGEM3-GC31 experiments. This dependence on the forcing can also contribute to the different resolution effect found in MPI-ESM, compared to HadGEM3-GC31 experiments.

Generally, when studying the effect of resolving ocean eddies on the climate response, one should pay attention not only to the resolution of the ocean model, but also that of the atmosphere model. While the atmospheric resolution should be increased when increasing oceanic resolution so that the ocean mesoscale structures can be "felt" by the atmosphere (Bryan et al., 2010), an increase in atmospheric resolution can also induce changes in climate feedback parameter in addition to the resolution effect due to ocean eddies. In this case, the resolution effect diagnosed from the experiments can include both that induced by resolving mesoscale eddies and that induced by modified climate feedbacks. The above considerations suggest a high sensitivity of the effect of resolving ocean eddies on GMST response to both the atmospheric model and the forcing scenario used. One should keep this in mind when verifying the results reported here using different climate models.

5.3. Possible Effect of Spurious Diapycnal Mixing

The result of this paper is based on the MPIOM as a z-level ocean model. Such a model has the tendency for the advection scheme to produce unphysical diapycnal mixing (Griffies et al., 2000; Lee et al., 2002; Megann, 2018), which can have adverse consequences for the representation of the heat uptake. The consideration of the energy budget of the coupled system suggests that the effect of the unphysical mixing is small, at least when integrated over the entire ocean. This is because the heat uptake of the entire ocean would otherwise be strongly distorted. The distortion would prevent the resolution effect of the heat uptake response to match that of GMST response - a quantity that includes the land surface temperature and is (under a strong GHG forcing) more strongly controlled by the GHG forcing than by the ocean's state. However, small in an integral sense does not mean small everywhere. It is possible that there exists some kind of mutual cancellation. It is also possible that the enhanced vertical mixing in response to strong vertical velocity fluctuations (shown in Figure S4) is related to spurious diapycnal mixing. All these questions and caveats need to be investigated elsewhere.

6. Conclusions

We use pairs of climate change experiments with the same atmosphere model coupled to an ocean model at two different resolutions to quantify the effect of resolved mesoscale eddies. The experiments are specially designed (a) to eliminate possible drifts in climate change simulations performed with an eddy-resolving ocean model, (b) to concentrate on the effect of ocean resolution only, and (c) to enhance signal-to-noise ratio - both by using an ensemble and by employing a strong forcing (i.e., 4xCO_2). We find the following:

1. Resolving mesoscale eddies has a small but energetically consistent impact on the transient response of GMST. It reduces the warming by about 0.1°C under a CO_2 quadrupling in MPI-ESM experiments
2. The weaker GMST response is related to a stronger heat uptake by the mid and deep ocean. The deep heat uptake occurs quickly after imposing the 4xCO_2 forcing and persists its strength over the whole integration period of 100 years, presumably due to vertical mixing related to vertical velocity fluctuations
3. Resolving eddies leads to a stronger deep ocean heat uptake, manifested in an intensification of the magnitude of all heat process responses

Generally, the effect of an eddying ocean on transient climate response should be studied by diagnosing the heat uptake of the entire ocean. One should not just focus on the upper ocean heat uptake to account for ocean's role in buffering the climate system against steep rise in surface temperatures, lending support for the deep ARGO float observation system to gather data and observe at such depths that are currently under-observed.

Data Availability Statement

Details of primary data for this study is available on http://hdl.handle.net/21.11116/0000-0008-3279-8. MPI-ESM-ER output data for this study is stored on long-term archive at DKRZ and made searchable from https://cera-www.dkrz.de/WDCC/ui/cerasearch/ with the keyword search "944". HadGEM data for this study is available through ESGF (http://cera-www.dkrz.de/WDCC/meta/CMIP6/CMIP6.HighResMIP.NERC.HadGEM3-GC31-HH).

Acknowledgments
This study is supported by PRIMAVERA, a Horizon 2020 project funded by the European Commission, with grant number 641727. The work is partly funded by the Deutsche Forschungsgemeinschaft (DFG, German Research Foundation) under Germany's Excellence Strategy - EXC 2037 "CLICCS - Climate, Climatic Change, and Society" - Project Number: 390683824. The authors thank the German Computing Centre (DKRZ) for providing the computational resources and the Max Planck Society for the Advancement of Science for their support. The authors also thank Veit Lüschow for providing insightful comments and suggestions to this manuscript.

References

Bryan, F. O., Tomas, R., Dennis, J. M., Chelton, D. B., Loeb, N. G., & McClean, J. L. (2010). Frontal scale air-sea interaction in high-resolution coupled climate models. *Journal of Climate*, *23*(23), 6277–6291. https://doi.org/10.1175/2010JCLI3665.1

Chelton, D. B., deSzoeke, R. A., Schlax, M. G., El Naggar, K., & Siwertz, N. (1998). Geographical variability of the first baroclinic rossby radius of deformation. *Journal of Physical Oceanography*, *28*(3), 433–460. https://doi.org/10.1175/1520-0485(1998)028⟨0433:GVOTFB⟩2.0.CO;2

Gent, P. R., & Mcwilliams, J. C. (1990). Isopycnal mixing in ocean circulation models. *Journal of Physical Oceanography*, *20*(1), 150–155. https://doi.org/10.1175/1520-0485(1990)020⟨0150:IMIOCM⟩2.0.CO;2

Geoffroy, O., Saint-Martin, D., Olivié, D. J. L., Voldoire, A., Bellon, G., & Tytéca, S. (2013). Transient climate response in a two-layer energy-balance model. part i: Analytical solution and parameter calibration using CMIP5 aogcm experiments. *Journal of Climate*, *26*(6), 1841–1857. https://doi.org/10.1175/JCLI-D-12-00195.1

Gregory, J. M., Ingram, W. J., Palmer, M. A., Jones, G. S., Stott, P. A., Thorpe, R. B., et al. (2004). A new method for diagnosing radiative forcing and climate sensitivity. *Geophysical Research Letters*, *31*(3), L03205. https://doi.org/10.1029/2003GL018747

Griffies, S. M., Pacanowski, R. C., & Hallberg, R. W. (2000). Spurious diapycnal mixing associated with advection in az-coordinate ocean model. *Monthly Weather Review*, *128*(3), 538–564. https://doi.org/10.1175/1520-0493(2000)128⟨0538:SDMAWA⟩2.0.CO;2

Griffies, S. M., Winton, M., Anderson, W. G., Benson, R., Delworth, T. L., Dufour, C. O., et al. (2015). Impacts on ocean heat from transient mesoscale eddies in a hierarchy of climate models. *Journal of Climate*, *28*(3), 952–977. https://doi.org/10.1175/JCLI-D-14-00353.1

Gutjahr, O., Putrasahan, D. A., Lohmann, K., Jungclaus, J. H., von Storch, J.-S., et al. (2019). Max Planck Institute Earth System Model (MPI-ESM1.2) for the High-Resolution Model Intercomparison Project (HighResMIP). *Geoscientific Model Development*, *12*(7), 3241–3281. https://doi.org/10.5194/gmd-12-3241-2019

Haarsma, R. J., Roberts, M. J., Vidale, P. L., Senior, C. A., Bellucci, A., Bao, Q., et al. (2016). High Resolution Model Intercomparison Project (HighResMIP v1.0) for CMIP6. *Geoscientific Model Development*, *9*(11), 4185–4208. https://doi.org/10.5194/gmd-9-4185-2016

Hallberg, R. (2013). Using a resolution function to regulate parameterizations of oceanic mesoscale eddy effects. *Ocean Modelling*, *72*, 92–103. https://doi.org/10.1016/j.ocemod.2013.08.007

IPCC. (2013), *Climate change 2013: The physical science basis. Contribution of working group I to the fifth assessment report of the intergovernmental panel on climate change* (T. F. Stocker, D. Qin, G.-K. Plattner, M. Tignor, S. K. Allen, J. Boschung, (Eds.). Cambridge, UK, NY, USA: Cambridge University Press.

Jungclaus, J. H., Fischer, N., Haak, H., Lohmann, K., Marotzke, J., Matei, D., et al. (2013). Characteristics of the ocean simulations in the Max Planck Institute Ocean Model (MPIOM) the ocean component of the MPI-Earth system model. *Journal of Advances in Modeling Earth Systems*. *5*, 422–446. https://doi.org/10.1002/jame.20023@10.1002/(ISSN)1942-2466

Lee, M.-M., Coward, A. C., & Nurser, A. J. G. (2002). Spurious diapycnal mixing of the deep waters in an eddy-permitting global ocean model. *Journal of Physical Oceanography*, *32*(5), 1522–1535. https://doi.org/10.1175/1520-0485(2002)032⟨1522:SDMOTD⟩2.0.CO;2

Liang, X., Spall, M., & Wunsch, C. (2017). Global ocean vertical velocity from a dynamically consistent ocean state estimate. *Journal of Geophysical Research: Oceans*, *122*(10), 8208–8224. https://doi.org/10.1002/2017JC012985

Mauritsen, T., Bader, J., Becker, T., Behrens, J., Bittner, M., Brokopf, R., et al. (2019). Developments in the MPI-M Earth System Model version 1.2 (MPI-ESM1.2) and its response to increasing CO_2. *Journal of Advances in Modeling Earth Systems*, *11*(4), 998–1038. https://doi.org/10.1029/2018MS001400

Megann, A. (2018). Estimating the numerical diapycnal mixing in an eddy-permitting ocean model. *Ocean Modelling*, *121*, 19–33. https://doi.org/10.1016/j.ocemod.2017.11.001

Mikolajewicz, T., & Gregory, J. M. (2012). Ocean heat uptake and its consequences for the magnitude of sea level rise and climate change. *Geophysical Research Letters*, *39*(18), L18608. https://doi.org/10.1029/2012GL052952

Morrison, A. K., Saenko, O. A., Hogg, A. M., & Spence, P. (2013). The role of vertical eddy flux in southern ocean heat uptake. *Geophysical Research Letters*, *40*(20), 5445–5450. https://doi.org/10.1002/2013GL057706

Müller, W. A., Jungclaus, J. H., Mauritsen, T., Baehr, J., Bittner, M., Budich, R., et al. (2018). A Higher-resolution Version of the Max Planck Institute Earth System Model (MPI-ESM1.2-HR). *Journal of Advances in Modeling Earth Systems*, *10*(7), 1383–1413. https://doi.org/10.1029/2017MS001217

Munk, W. (1966). Abyssal recipes. *Deep-Sea Research and Oceanographic Abstracts*, *13*(4), 707–730. https://doi.org/10.1016/0011-7471(66)90602-4

Munk, W., & Wunsch, C. (1998). Abyssal recipes II: Energetics of tidal and wind mixing. *Deep Sea Research I: Oceanographic Research Papers*, *45*(12), 1977–2010. https://doi.org/10.1016/S0967-0637(98)00070-3

Nurser, A. J. G., & Bacon, S. (2014). The Rossby radius in the Arctic Ocean. *Ocean Science*, *10*(6), 967–975. https://doi.org/10.5194/os-10-967-2014

O'Neill, B. C., Tebaldi, C., van Vuuren, D. P., Eyring, V., Friedlingstein, P., Hurtt, G., et al. (2016). The scenario model intercomparison project (scenariomip) for CMIP6. *Geoscientific Model Development*, *9*(9), 3461–3482. https://doi.org/10.5194/gmd-9-3461-2016

Redi, M. H. (1982). Oceanic isopycnal mixing by coordinate rotation. *Journal of Physical Oceanography*, *12*(10), 1154–1158. https://doi.org/10.1175/1520-0485(1982)012⟨1154:OIMBCR⟩2.0.CO;2

Roberts, M. J., Baker, A., Blockley, E. W., Calvert, D., Coward, A., Hewitt, H. T., et al. (2019). Description of the resolution hierarchy of the global coupled HadGEM3-GC3.1 model as used in CMIP6 HighResMIP experiments. *Geoscientific Model Development*, *12*(12), 4999–5028. https://doi.org/10.5194/gmd-12-4999-2019

Rose, B. E. J., & Rayborn, L. (2016). The effects of ocean heat uptake on transient climate sensitivity. *Current Climate Change Reports*, *2*(4), 190–201. https://doi.org/10.1007/s40641-016-0048-4

Saenko, O. A., Yang, D., & Gregory, J. M. (2018). Impact of mesoscale eddy transfer on heat uptake in an eddy-parameterizing ocean model. *Journal of Climate*, *31*(20), 8589–8606. https://doi.org/10.1175/JCLI-D-18-0186.1

Stevens, B., Giorgetta, M., Esch, M., Mauritsen, T., Crueger, T., Rast, S., et al. (2013). Atmospheric component of the MPI-M Earth System Model: ECHAM6. *Journal of Advances in Modeling Earth Systems*, *5*(2), 146–172. https://doi.org/10.1002/jame.20015

von Storch, H., & Zwiers, F. W. (1999). *Statistical analysis in climate Research*. Cambridge University Press. https://doi.org/10.1017/CBO9780511612336

von Storch, J.-S., Haak, H., Hertwig, E., & Fast, I. (2016). Vertical heat and salt fluxes due to resolved and parameterized meso-scale eddies. *Ocean Modelling*, *108*, 1–19. https://doi.org/10.1016/j.ocemod.2016.10.001

Winton, M., Anderson, W. G., Delworth, T. L., Griffies, S. M., Hurlin, W. J., & Rosati, A. (2014). Has coarse ocean resolution biased simulations of transient climate sensitivity? *Geophysical Research Letters*, *41*(23), 8522–8529. https://doi.org/10.1002/2014GL061523

Winton, M., Takahashi, K., & Held, I. M. (2010). Importance of ocean heat uptake efficacy to transient climate change. *Journal of Climate*, *23*(9), 2333–2344. https://doi.org/10.1175/2009JCLI3139.1

Wolfe, C. L., Cessi, P., McClean, J. L., & Maltrud, M. E. (2008). Vertical heat transport in eddying ocean models. *Geophysical Research Letters*, *35*(23), L23605. https://doi.org/10.1029/2008GL036138